

# Mitochondrial Respiratory Dysfunction Induces Claudin-1 Expression via Reactive Oxygen Species-mediated Heat Shock Factor 1 Activation, Leading to Hepatoma Cell Invasiveness\*

Received for publication, March 26, 2015, and in revised form, July 7, 2015. Published, JBC Papers in Press, July 8, 2015, DOI 10.1074/jbc.M115.654913

Jong-Hyuk Lee<sup>‡§1</sup>, Young-Kyoung Lee<sup>‡§1</sup>, Jin J. Lim<sup>‡§1</sup>, Hae-Ok Byun<sup>‡§</sup>, Imkyong Park<sup>‡§</sup>, Gyeong-Hyeon Kim<sup>‡§</sup>, Wei Guang Xu<sup>¶</sup>, Hee-Jung Wang<sup>¶</sup>, and Gyesoon Yoon<sup>‡§2</sup>

From the Departments of <sup>‡</sup>Biochemistry and <sup>¶</sup>Surgery, Ajou University School of Medicine, Suwon, 443-380, Korea and the <sup>§</sup>Department of Biomedical Science, Graduate School, Ajou University, Suwon 443-380, Korea

**Background:** Increased claudin-1 (Cln-1) expression in human hepatoma cells with mitochondrial defects leads to high tumor cell invasiveness.

**Results:** Cln-1-mediated hepatoma cell invasiveness occurs via heat shock factor 1 (HSF1) activation.

**Conclusion:** The mitochondrial defect-ROS-HSF1 axis controls hepatoma cell invasiveness.

**Significance:** HSF1 is a key mitochondrial retrograde-responsive transcription factor controlling hepatoma cell invasiveness.

Although mitochondrial dysfunction has been implicated in tumor metastasis, it is unclear how it regulates tumor cell aggressiveness. We have reported previously that human hepatoma cells harboring mitochondrial defects have high tumor cell invasion activity via increased claudin-1 (Cln-1) expression. In this study, we demonstrated that mitochondrial respiratory defects induced Cln-1 transcription via reactive oxygen species (ROS)-mediated heat shock factor 1 (HSF1) activation, which contributed to hepatoma invasiveness. We first confirmed the inverse relationship between mitochondrial defects and Cln-1 induction in SNU hepatoma cells and hepatocellular carcinoma tissues. We then examined five different respiratory complex inhibitors, and complex I inhibition by rotenone most effectively induced Cln-1 at the transcriptional level. Rotenone increased both mitochondrial and cytosolic ROS. In addition, rotenone-induced Cln-1 expression was attenuated by *N*-acetylcysteine, an antioxidant, and exogenous H<sub>2</sub>O<sub>2</sub> treatment was enough to increase Cln-1 transcription, implying the involvement of ROS. Next we found that ROS-mediated HSF1 activation via hyperphosphorylation was the key event for Cln-1 transcription. Moreover, the Cln-1 promoter region (from –529 to +53) possesses several HSF1 binding elements, and this region showed increased promoter activity and HSF1 binding affinity in response to rotenone treatment. Finally, we demonstrated that the invasion activity of SNU449 cells, which harbor mitochondrial defects, was blocked by siRNA-mediated HSF1 knockdown. Taken together, these results indicate that mitochondrial respiratory defects enhance Cln-1-mediated hepatoma cell invasiveness via mitochondrial ROS-mediated HSF1

activation, presenting a potential role for HSF1 as a novel mitochondrial retrograde signal-responsive transcription factor to control hepatoma cell invasiveness.

Mitochondrial respiratory defects are distinct metabolic features of cancer cells (1, 2). In the early stages of cancer development, actively proliferating tumor cells cannot avoid hypoxia because of their rapid nodular mass formation. Therefore, this respiratory impairment has long been recognized as an epiphenomenon of tumors. However, mitochondrial defects and the accompanying activated glycolysis persist in metastatic malignant cancers even after a normoxic environment is restored by activated angiogenesis. Similar observations have been made with cultivated tumor cells under normoxia (3), indicating that cancerous respiratory defects are not just a transient consequence of environmental constraints in tumor tissue but may be the result of genetic changes or oncogenic modulations. Indeed, the mitochondrial defects found in cancer cells are mostly associated with mitochondrial DNA damage, such as deletions and/or point mutations, as described in many types of cancers (4–7). Mitochondrial dysfunction is also induced by oncogenic Myc-mediated pyruvate dehydrogenase inactivation (8) or by oncogenic Ras-mediated mitophagic degradation (9). Interestingly, mitochondrial DNA damage or mitochondrial defects may contribute to cancer promotion, metastasis, and chemoresistance in addition to primary tumor growth (6, 10–12). These observations suggest that mitochondrial defects have causative roles in tumor progression. However, the underlying molecular mechanisms of how mitochondrial dysfunction regulates tumor progression are not fully understood.

Increased levels of reactive oxygen species (ROS)<sup>3</sup> and the resultant oxidative stress are also key features of tumor cells. Cancer cells with a high metastasis capacity have more ROS accumulation than those with a low tendency for metastasis

\* This work was supported by National Research Foundation of Korea Grants NRF-2012R1A5A2048183 and NRF-2012R1A2A2A01043185 funded by the Korean government (MSIP). The authors declare that they have no conflicts of interest with the contents of this article.

The amino acid sequence of this protein can be accessed through NCBI Protein Database under NCBI accession number NG\_021418.

<sup>1</sup> These authors contributed equally to this work.

<sup>2</sup> To whom correspondence should be addressed: Dept. of Biochemistry, Ajou University School of Medicine, Suwon 443-721, Korea. Tel.: 82-31-219-5054; Fax: 82-31-219-5059; E-mail: ypeace@ajou.ac.kr.

<sup>3</sup> The abbreviations used are: ROS, reactive oxygen species; HCC, hepatocellular carcinoma; OCR, oxygen consumption rate; NAC, *N*-acetylcysteine; HSE, heat shock element.

## Mitochondrially Mediated HSF1 Activation Induces Cln-1

(13–15). In addition to ROS-induced oxidative damage to cellular proteins, lipids, and nucleotides, ROS also function as second messengers to regulate various metastasis-related signaling pathways via reversible oxidative posttranslational modifications (16), subsequently contributing to tumor angiogenesis, cancer cell invasiveness, and metastasis. Interestingly, increased ROS in cancer cells emanate primarily from defective mitochondria as a result of an incomplete and inefficient electron transfer process in the defective respiratory chains (17–19), supporting the mechanistic link between tumor progression and mitochondrial defects. Inhibition of complex I activity by stable suppression of GRIM-19 or NDUFS3 decreased complex I-enhanced cell migration, invasion, and spheroid formation through ROS production (10). The contribution of mitochondrial dysfunction-mediated ROS to cell migration activity was also demonstrated in SC-M1 human gastric cancer cells (20). These observations emphasize the key role of ROS in mitochondrial dysfunction-mediated tumor progression.

Claudins are a family of tight junction components that form paracellular barriers, thereby controlling the flow of molecules in the intercellular space of the epithelium. However, aberrant up-regulation of claudins has often been reported in human cancers, including hepatocellular carcinoma (HCC) and primary colon carcinoma (21, 22). Among claudins, claudin-1 (Cln-1) is known to play a key role in the invasive behavior of human liver cells via the c-Abl-PKC signaling pathway (23). Overexpression of Cln-1 augments the invasiveness of tumor cells through increased secretion and activation of metalloproteinases (24, 25), which supports the tumor-promoting activity of Cln-1. Recently, we reported that hepatoma cells harboring mitochondrial dysfunction control cell invasion activity through augmenting Cln-1 expression. However, the molecular mechanism of how mitochondrial dysfunction controls Cln-1 expression remains unclear. In this study, we demonstrate that mitochondrial respiratory defects augment Cln-1 expression through ROS-mediated heat shock factor 1 (HSF1) activation, contributing to hepatoma cell invasiveness.

### Experimental Procedures

**Cell Cultures and Tumor Samples**—Human hepatoma cells (SNU-354, SNU-387, SNU-423, and SNU-449) were purchased from the Korean Cell Line Bank (Seoul, Korea) and cultured in Gibco RPMI 1640 medium (Invitrogen) supplemented with 10% Gibco FBS (Invitrogen) and Gibco antibiotics (Invitrogen) at 37 °C in a humidified incubator with 5% CO<sub>2</sub>. Chang cells were obtained from the ATCC. Chang cell clones were isolated by single-cell dilution and expansion of Chang cell (ATCC, Rockville, MD), and a Chang clone with strong hepatic characteristics (Ch-L), validated by confirming liver-specific expression of albumin and carbamoyl-phosphate synthase-1, was used for this study (26). Ch-L clones were cultured in Gibco DMEM (Invitrogen) supplemented with 10% FBS.

HCC tumor samples and surrounding control tissues were obtained from 28 patients with HCC during the period of 2003–2005 at Ajou University Hospital after surgical resection with informed consent through the Ajou Institutional Review Board. No patient in this study received chemotherapy or radiation therapy before surgery.

**Measurement of the Oxygen Consumption Rate (OCR)**—The OCR was also measured *in situ* with cultured cells using an XF-24 extracellular flux analyzer (Seahorse Bioscience, North Billerica, MA) according to the protocol provided. Briefly, cells were seeded on XF24 cell culture microplates (Seahorse Bioscience) at a density of 10,000 cells/well and preincubated with XF assay medium (Seahorse Bioscience) containing 1 mM pyruvate and 5 mM glucose. Its mitochondrial specificity was confirmed by adding 5 mM KCN.

**Immunocytochemistry**—Cells were fixed with 4% paraformaldehyde, permeabilized with 0.3% Triton X-100 for 10 min, and incubated in blocking solution (2% bovine serum albumin in TBS containing 0.1% Tween 20) for 2 h. After incubation overnight with primary antibody for Cln-1 (catalog no. 717800, Invitrogen) at 4 °C, cells were washed three times and probed with cy3-conjugated anti-rabbit antibody (Jackson ImmunoResearch Laboratories, West Grove, PA) for 1 h. After washing and mounting with mounting solution, cells were visualized by confocal microscope (LSM710, Carl Zeiss, Oberkochen, Germany).

**Estimation of Intracellular and Mitochondrial ROS Levels**—To determine intracellular and mitochondrial ROS levels, dichlorofluorescein diacetate (Molecular Probes, Eugene, OR) and mitochondrial specific MitoSOX<sup>®</sup> (Invitrogen) fluorogenic probes were used, respectively (27). Briefly, cells were incubated in media containing dichlorofluorescein diacetate (20 μM) and MitoSOX<sup>®</sup> (25 μM) for 20 min at 37 °C. Stained cells were washed, resuspended in PBS, and analyzed by flow cytometry (FACS Vantage, BD Biosciences). Mean values of arbitrary fluorescence units of 10,000 cells were used and expressed as the percentage of negative control.

**Subcellular Fractionation**—The nuclear and cytoplasmic fractions were obtained from 90% confluent grown cells on 100-mm dishes as described previously with slight modifications (28). Briefly, cells were harvested by trypsinization and resuspended in medium A (250 mM sucrose, 0.1 mM EDTA, and 2 mM HEPES (pH 7.4)). The cell slurry was homogenized in a Dounce homogenizer (StedFast<sup>™</sup> stirrer, Fisher Scientific, Pittsburgh, PA) and spun at 500 rcf for 10 min to precipitate nuclei. The nucleus pellets were washed three times with buffer A (0.1 mM EDTA, 10 mM KCl, and 10 mM HEPES (pH 7.9)) containing 1% Nonidet P-40, and the final pellets were collected for the nucleus fraction. The supernatant cytoplasmic fractions were separately collected. Nucleus and cytoplasmic fractions were subjected to lysis in radioimmune precipitation assay buffer (150 mM NaCl, 1% Nonidet P-40, 0.5% sodium deoxycholate, 0.1% sodium dodecyl sulfate, and 50 mM Tris (pH 8.0)) for Western blot analysis.

**Construction of HSF1 cDNA Plasmids and Transfection of cDNA Plasmids and siRNAs**—To generate a cDNA plasmid, pcDNA-HSF1-HA, conventional cloning procedures were applied. Briefly, the pcDNA-HSF1-HA plasmid was constructed by conventional TA cloning using pGEMT-easy (Promega), and the HSF1 cDNA fragment was amplified by PCR using total cDNAs of the Ch-L clone and the primer set 5'-AGAATTCATGGATCTGCCCG and 5'-TGAGCTCGGAGACAGTGGG. The HSF1 cDNA was subcloned into EcoRI and XhoI sites of the pcDNA3-HA vector constructed

previously (29). The Cln-1 overexpression plasmid pcDNA-Cln-1 has been constructed previously (26).

To introduce plasmids and siRNAs into cells, cells were transfected with plasmids and siRNA duplexes using FuGENE HD (Promega) and Oligofectamine<sup>TM</sup> reagent (Invitrogen), respectively, according to the instructions of the manufacturer. HSF1 siRNAs (#1, 5'-ACUGUAGAUUGCUUCUGUA; #2, 5'-GAACUAAAGCCAAGGGUUAU) and negative control siRNAs (5'-CCUACGCCACCAAUUUCGU) were obtained from Bioneer (Seoul, Korea).

**Construction of the Promoter-Luciferase Reporter Plasmid and Promoter Assay**—The human *Cln-1* promoter region of 767 bp (−529 to +238, NG\_021418) was cloned by targeted PCR against total genomic DNA of Ch-L using a primer set, 5'-GCTCGAGCCAATCTGTAGAGTGT and 5'-TATAGATCTTCGCTCGGGCGC. The amplified *Cln-1* promoter region was inserted between the BglII and XhoI sites of the pGL3-basic vector (Promega). After construction, the inserted promoter was confirmed by DNA sequencing.

To monitor *Cln-1* promoter activity, cells were transfected with a total of 1 μg of DNA (700 ng of pcDNA3 or pcDNA3-HSF1-HA, 250 ng of the cloned reporter plasmid, and 50 ng of thymidine kinase promoter-driven *Renilla* luciferase plasmid as an internal control) using FuGENE HD reagent. After 2 days, the luciferase activity of the cell lysate was measured by Synergy 2 multi-mode reader (BioTek Instruments, Inc., Winooski, VT) according to the protocol provided with the Dual-Luciferase reporter assay system (Promega). The *Cln-1* promoter-mediated luciferase activities of the reporter plasmid were normalized to *Renilla* luciferase activity.

**ChIP Assay**—The ChIP assay was performed according to the ChIP assay kit protocol (Upstate Biotechnology Inc., Lake Placid, NY) with slight modifications. Briefly, cells were treated with 1% formaldehyde to stably cross-link the DNA-interacting proteins to genomic DNA. After lysis, the lysates were sonicated briefly to shear genomic DNA and centrifuged at 13,000 rpm for 10 min. An aliquot was saved for input control, and the other aliquots were subjected to ChIP using HSF1 antibody (catalog no. 4356S, Cell Signaling Technology) and protein G-agarose beads (Millipore Corp., Billerica, MA). The eluted DNA was purified using a DNA extraction kit (Inclone Biotech, Seoul, Korea), and the specific *Cln-1* promoter region (−490 to +53, 543 bp) was amplified by PCR with the primer sets 5'-GAGACAAGTGATGGAACGACC and 5'-CTGGAGTCTG-GATACTAGAAGC (Bioneer) and sequenced for validation.

**Cell Invasion Assay**—Cell invasion assays were performed with Transwell® permeable supports (Corning, Acton, MA) according to the instructions of the manufacturer. Briefly, cells ( $2 \times 10^4$ ) prestarved with serum-free RPMI for 16 h were placed into the upper chamber with 0.2 ml of serum-free RPMI. RPMI (0.8 ml) supplemented with 10% fetal bovine serum was placed in the lower chamber as a chemoattractant. Uncoated porous filters (8-μm pore size) were precoated with 7% growth factor-reduced BD Matrigel<sup>TM</sup> matrix (BD Biosciences) for the assay. The cells invading the lower surface were fixed by 100% methanol for 1 min, stained with hematoxylin solution (Sigma-Aldrich, St. Louis, MI) and eosin Y solution (Sigma-Aldrich) and

counted. All experiments were performed as independent triplicate experiments.

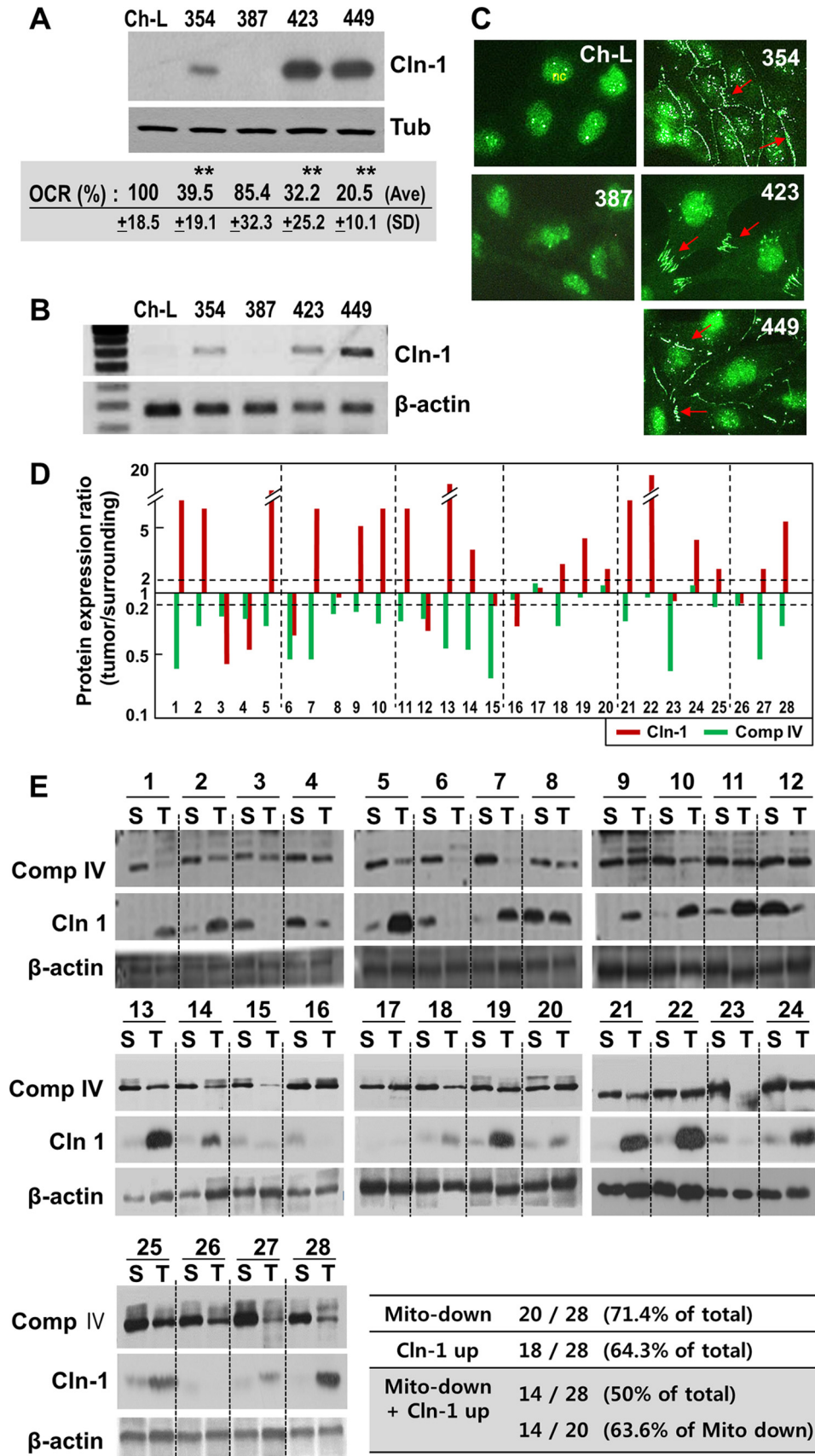
**Western Blot Analysis**—Western blotting was performed using standard procedures. Cln-1 antibody (catalog no. 717800) was purchased from Invitrogen, and HSF1 antibody (catalog no. 4356S) was from Cell Signaling Technology. Antibody for phospho-HSF1 (Ser(P)-326, catalog no. ab115702) was obtained from Abcam. Antibodies for β-actin (catalog no. sc-1616) and α-tubulin (catalog no. sc-5286) were from Santa Cruz Biotechnology. Antibodies against NDUFA9 of complex I (catalog no. A21344) and MTCOII of complex IV (catalog no. A6404) were from Molecular Probes.

**RT-PCR**—Total RNA was isolated using TRIzol (Invitrogen), and cDNA was prepared using avian myeloblastosis virus reverse transcriptase (Promega). PCR was performed with 25–30 cycles of the reaction involving 95 °C for 30 s, 53–58 °C for 30 s, and 72 °C for 70–90 s. The PCR primer sets for Cln-1 (5'-GAGCGAGTCATGGCCAACGCG and 5'-GCCTCTGT-GTCACACGTAGTC), NDUFA3 (5'-CAGTGCTGGTCGTG-TCCCTC and 5'-GGCATGTTCCCATCATCACG), UQCRB (5'-GCCTTTCTCTGTTGCGCATG and 5'-ATCCAGCCAC-TTGCTGATG), ATP5G3 (5'-TCTCGACCAGAGGCTAG-TAGG and 5'-TTGCAGCACCTGCACCAATA), and β-actin (5'-CCTTCCTGGGCATGGAGTCTGT and 5'-GGAGCA-ATGATCTTGATCTTC for a short fragment of 202 bp and 5'-GCACTCTTCCAGCCTTCTT and 5'-CTGTACCTT-CACCGTTCCA for a long fragment of 518 bp) were produced by Bioneer. Quantitative real-time RT-PCR was performed by using Thunderbird<sup>TM</sup> SYBR<sup>TM</sup> quantitative PCR mix (Toyobo Co., Ltd., Osaka, Japan) and the Bio-Rad CFX96<sup>TM</sup> real-time system.

## Results

**Increased Expression of Cln-1 Is Associated with Mitochondrial Dysfunction of Hepatoma Cells**—First we examined the relationship between mitochondrial dysfunction and Cln-1 expression in hepatoma cells using four different SNU hepatoma cells (SNU-354, SNU-387, SNU-423, and SNU449). A previously characterized Ch-L clone that possesses liver-specific genes (30) was used as a control with active mitochondria. SNU-354, SNU-423, and SNU449 cells with defective mitochondrial respiration showed increased Cln-1 expression at both the mRNA and protein levels, whereas cells with active mitochondria (SNU387 and the Ch-L clone) had low Cln-1 expression (Fig. 1, A and B). Increased Cln-1 expression was mostly localized in the cell-to-cell contact region of the plasma membrane (Fig. 1C), implying its usual function as a tight junction component. Next, we compared the expression levels of Cln-1 and a core subunit of mitochondrial respiratory complex IV using 28 individual HCC tumor samples and their surrounding specimens (Fig. 1, D and E). There was no clear one-on-one correlation between decreased complex IV subunit and increased Cln-1 expression in human hepatoma tissues. However, 20 tumor samples had decreased expression (below 0.2-fold) of the complex IV subunit, implying mitochondrial defects. Of 20 samples with mitochondrial defects, 14 (63.6%) had increased expression (more than 2.0-fold induction) of Cln-1 (Fig. 1E). These results suggest that up-regulation of

# Mitochondrially Mediated HSF1 Activation Induces Cln-1



Cln-1 expression may be associated with mitochondrial dysfunction in some hepatoma cells.

**Complex I Inhibition by Rotenone Effectively Induces Cln-1 Expression at the Transcriptional Level**—Next we investigated the relationship between Cln-1 expression and mitochondrial defects. Overexpression of Cln-1, regardless of whether it was transient or stable, in Ch-L clones did not affect the OCR (Fig. 2, A and B). However, when Ch-L clones were treated with the respiratory inhibitors rotenone (complex I inhibitor), thenoyltrifluoroacetone (complex II inhibitor), antimycin A (complex III inhibitor), and oligomycin (complex V inhibitor), Cln-1 expression was increased significantly at the transcription level without altering respiratory subunit expression or any clear alterations in respiratory subunit expression (data not shown). KCN (complex IV inhibitor) did not lead to increased Cln-1 expression (Fig. 2, C and D). Of the five respiratory complex inhibitors, complex I inhibition by rotenone showed the most effective Cln-1 induction. This induction started with 1  $\mu$ M rotenone and increased progressively 3 h after treatment at the transcription level (Fig. 2, E and F). We further demonstrated that a mitochondrial defect by siRNA-mediated knockdown of NDUFA9, a complex I subunit, induced Cln-1 expression (Fig. 2G). These results indicate that the mitochondrial complex I defect is involved in Cln-1 expression and also suggest that rotenone-induced Cln-1 expression can be used as a proper model to elucidate the molecular link between mitochondrial defects and Cln-1 expression.

**Mitochondrial ROS Generated by Rotenone Are a Key Regulator of Cln-1 Expression**—Next we asked how complex I inhibition by rotenone regulated Cln-1 transcription. To address this, we monitored intracellular and mitochondrial ROS levels in hepatoma cells and compared them with those of Ch-L clones. Hepatoma cells with mitochondrial defects had increased levels of both mitochondrial and intracellular ROS (Fig. 3A). When the Ch-L clone was treated with rotenone, both mitochondrial and intracellular ROS increased in a dose-dependent manner, accompanying Cln-1 mRNA induction and showing an inverse relationship with respiratory inhibition (Fig. 3B). Pretreatment with *N*-acetylcysteine (NAC), an antioxidant, effectively blocked rotenone-induced Cln-1 transcription (Fig. 3C). When the Ch-L clone was exposed to a subcytotoxic dose of hydrogen peroxide ( $H_2O_2$ ), intracellular ROS increased in a biphasic manner, and mitochondrial ROS increased progressively (Fig. 3, Da and Fa), implying that the second peak of intracellular ROS may be linked with mitochondrial ROS, which was probably triggered by an  $H_2O_2$ -induced mitochondrial defect (Fig. 3F, b). This biphasic ROS generation by a subcytotoxic dose of  $H_2O_2$  corresponds well with a previous report (31). Interestingly, under these conditions, Cln-1 mRNA expression also showed a biphasic profile, suggesting

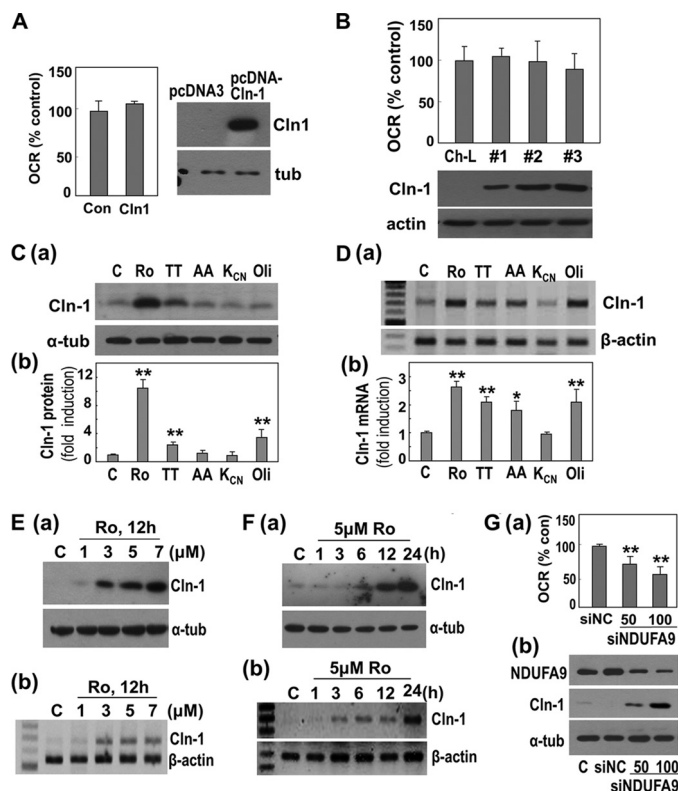


**FIGURE 2. Pharmacological inhibition of respiratory complex I effectively induces Cln-1 expression at the transcriptional level.** A, OCR was measured after Cln-1 was overexpressed in the Ch-L clone using pcDNA-Cln-1. Con, control; tub, tubulin. B, Ch-L clones stably expressing Cln-1 were isolated after transfecting cells with the pcDNA-Cln-1 plasmid and then subjected to an OCR assay (top panel) and Western blot analysis (bottom panel). C and D, the Ch-L clone was challenged with 5  $\mu$ M rotenone (Ro), 200  $\mu$ M thenoyltrifluoroacetone (TT), 5  $\mu$ M antimycin A (AA), 5 mM KCN ( $K_{CN}$ ), or 5  $\mu$ M oligomycin (Oli) for 12 h. C, a representative Western blot image for Cln-1 (a) and quantified results (b) are shown. C, control. D, Cln-1 mRNA levels by RT-PCR. A representative gel image (a) and quantified results (b) are shown. E, the Ch-L clone was exposed to the indicated concentration of rotenone for 12 h. Western blot (a) and RT-PCR (b) results are shown. F, the Ch-L clone was challenged with 5  $\mu$ M rotenone for the indicated time periods. Western blot (a) and RT-PCR (b) results are shown. G, the Ch-L clone was transfected with siRNA (50 or 100 pmol) for NDUFA9 for 3 days and subjected to OCR measurement (a) and Western blot analysis (b). \*,  $p < 0.05$ ; \*\*,  $p < 0.01$  versus control by Student's *t* test.

that a certain level of ROS may be required for Cln-1 induction (Fig. 3, D and E). These results indicate that mitochondrial ROS generated by complex I inhibition is critically involved in Cln-1 transcription.

**ROS-mediated HSF1 Phosphorylation Is a Key Regulatory Event for Cln-1 Expression**—To investigate how mitochondrial ROS modulate Cln-1 expression, we analyzed potential transcription factor binding sites in the Cln-1 promoter region (−2729 to +271 bp, NCBI accession no. NG\_021418) using the TFSEARCH program. The most abundant transcription bind-

**FIGURE 1. The inverse relationship between Cln-1 expression and mitochondrial respiratory defects in hepatoma cells and tissues.** The Ch-L clone and SNU hepatoma cell lines (SNU354, SNU387, SNU4231, and SNU449) were cultured for 2 days to maintain an exponentially growing state. A, Cln-1 protein levels by Western blot analysis. OCRs of the cells were measured as described under "Experimental Procedures," and their percentages of control (Ch-L) are shown in the bottom panel. \*\*,  $p < 0.01$  versus Ch-L by Student's *t* test. Tub, tubulin. B, Cln-1 mRNA levels by RT-PCR. C, immunocytochemistry for detecting the intracellular localization of Cln-1. Arrows indicate enhanced expression of Cln-1 in the cell-to-cell contact regions of the cytoplasmic membrane. D, protein expression ratios of Cln-1 and the complex IV (Comp IV) subunit in 28 HCC tumor samples and their surrounding tissues from the Western blot analysis shown in E. E, Western blot analysis of 28 HCC tumors (T) and their surrounding specimens (S). Shown are numbers of tumor samples with down-regulated mitochondrial activity (Mito-down, <0.2-fold), which were estimated by complex IV subunit expression, with up-regulated Cln-1 expression (Cln-1 up, >2-fold induction), and with both Mito-down plus Cln-1 up.

## Mitochondrially Mediated HSF1 Activation Induces Cln-1

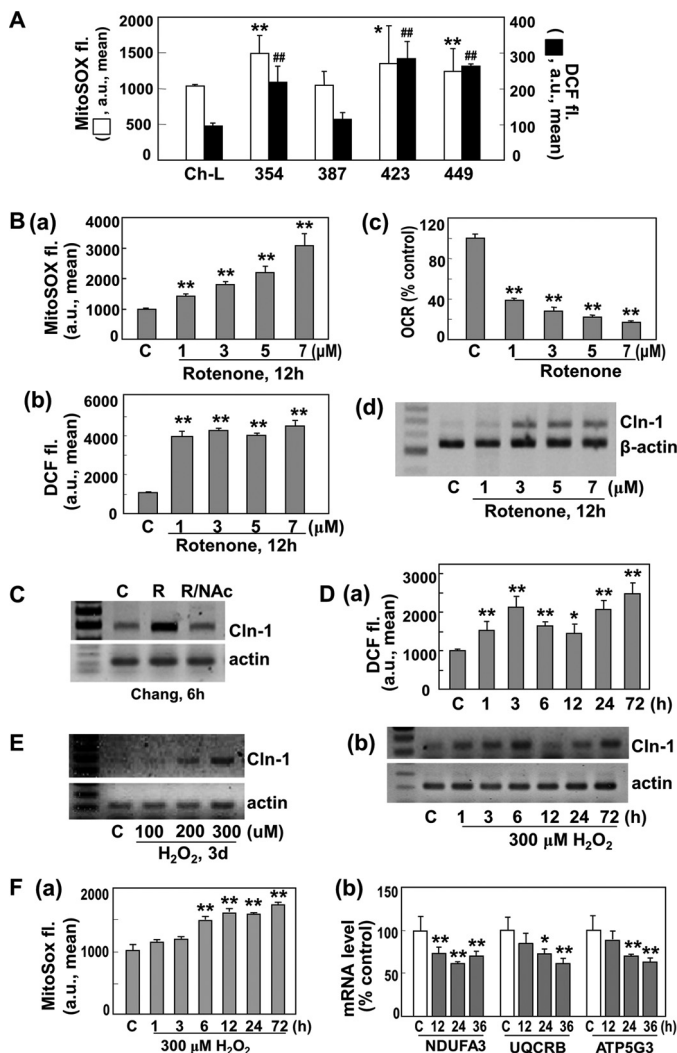


**FIGURE 3. Complex I inhibition-induced Cln-1 expression is mediated by ROS production.** *A*, the Ch-L clone and SNU hepatoma cell lines (SNU354, SNU387, SNU423, and SNU449) were cultured for 2 days to maintain an exponentially growing state. Mitochondrial and cytoplasmic ROS levels were measured by cytofluorimetric analysis after staining cells with MitoSOX (□) or dichlorofluorescein diacetate (■) fluorogenic (fl.) dyes, respectively. *B*, the Ch-L clone was treated with the indicated concentrations of rotenone for 12 h. Mitochondrial ROS levels (*a*), intracellular ROS levels (*b*), OCR (*c*), and Cln-1 mRNA levels by RT-PCR were monitored. *C*, control. *C*, the Ch-L clone was challenged with 5 μM rotenone for 12 h with or without NAC pretreatment for 6 h. Cln-1 mRNA levels were examined by RT-PCR. *D*, the Ch-L clone was exposed to 300 μM H<sub>2</sub>O<sub>2</sub> for the indicated time periods. Intracellular ROS levels (*a*) and mRNA levels (*b*) are shown. *E*, RT-PCR for Cln-1 was performed after the Ch-L clone was treated with the indicated concentrations of H<sub>2</sub>O<sub>2</sub> for 3 days. *F*, the Ch-L clone was exposed to 300 μM H<sub>2</sub>O<sub>2</sub> for the indicated time periods. Mitochondrial ROS levels (*a*) and mRNA levels of some respiratory complex subunits by quantitative RT-PCR (*b*) are shown. \*,  $p < 0.05$ ; \*\*,  $p < 0.01$  versus control by Student *t* test.

ing site in the promoter region was for HSF1, which is known as a stress-responsive transcription factor (data not shown) that is regulated by oxidative signaling (32), suggesting its potential involvement in mitochondrial ROS-mediated Cln-1 transcription. Upon exposure to rotenone, the mobility of the HSF1 protein band was delayed on SDS-PAGE (Fig. 4A), and this band was hyperphosphorylated, as shown by complete dephosphorylation using λ phosphatase (Fig. 4B). This finding implied that it was activated, as shown previously (33). The delayed band was phosphorylated on Ser-326 (Fig. 4A), the activating phos-

phorylation site (34). Rotenone-induced HSF1 activation was further demonstrated by augmented transcription of HSP70, a known major target of HSF1 (Fig. 4C) and nuclear targeting of HSF1 (Fig. 4D). HSP70 transcription was faster than Cln-1 transcription (Fig. 2F, *b*), implying differential regulation by HSF1. The delayed HSF1 mobility was recovered by NAC pretreatment and induced by exogenous H<sub>2</sub>O<sub>2</sub> treatment, corresponding with the Cln-1 expression pattern (Fig. 4, *E* and *F*). We then investigated whether rotenone-induced Cln-1 expression was truly mediated through HSF1. Induction of Cln-1 by rotenone was effectively suppressed by siRNA-mediated HSF1 knockdown, and HSF1 overexpression was sufficient to induce Cln-1 in the Ch-L clone (Fig. 4, *G* and *H*). These results support the hypothesis that complex I inhibition by rotenone induced Cln-1 transcription through ROS-mediated HSF1 activation.

**Complex I Inhibition Increases Cln-1 Promoter Activity through HSF1 Binding on the Promoter**—We then examined how HSF1 regulated Cln-1 transcription. We constructed a reporter plasmid containing the Cln-1 promoter region, including the transcription start, from -529 to +238. This promoter region contains more than 15 potential HSF1 binding sites (Fig. 5A). The cloned promoter region was sufficient for activation by rotenone treatment, and increased promoter activity was diminished by NAC pretreatment (Fig. 5, *B* and *C*). Overexpression of HSF1 itself increased promoter activity, and additional rotenone treatment further enhanced the activity but led to only a minor increase (Fig. 5D). We further demonstrated that complex I inhibition truly increased HSF1 binding to the Cln-1 promoter region (from -529 to +53) using a ChIP assay (Fig. 5E).

**HSF1 Activation Regulates Hepatoma Cell Invasiveness**—Finally, we investigated whether HSF1 activation induced by mitochondrial ROS is truly involved in hepatoma cell invasiveness. SNU hepatoma cells (SNU354, SNU423, and SNU449) harboring high Cln-1 expression and mitochondrial ROS had high cell invasion activity, and this invasiveness was blocked significantly by Cln-1 suppression but not completely (Fig. 6, *A* and *B*). Cln-1 overexpression- and NDUFA9 knockdown-mediated Cln-1 induction in the Ch-L clone also enhanced cell invasion activity (Fig. 6C), implying the involvement of mitochondrial defect-mediated Cln-1 expression in hepatoma cell invasiveness. Furthermore, cell lines harboring high Cln-1 expression showed delayed HSF1 mobility on SDS-PAGE (Fig. 6A). However, SNU354 cells had low expression of both HSF1 and Cln-1 without activating phosphorylation of Ser-326, whereas SNU423 and SNU449 cells had high HSF1 phosphorylation and Cln-1 expression (Fig. 6A). Unexpectedly, the invasion activity of SNU423 was not altered by HSF1 knockdown (data not shown), suggesting the possible involvement of additional inhibitory mechanisms on HSF1 activity in this cell. Therefore, we employed SNU449 cells to evaluate the role of HSF1 in hepatoma cell invasiveness. The high Cln-1 expression in SNU449 cells was obviously diminished by NAC treatment and siRNA-mediated HSF1 knockdown (Fig. 6, *D* and *Ea*). Eventually, siRNA-mediated HSF1 knockdown significantly decreased the invasion activity of SNU 449 cells (Fig. 6E, *b*). Taken together, these results indicate that ROS-mediated

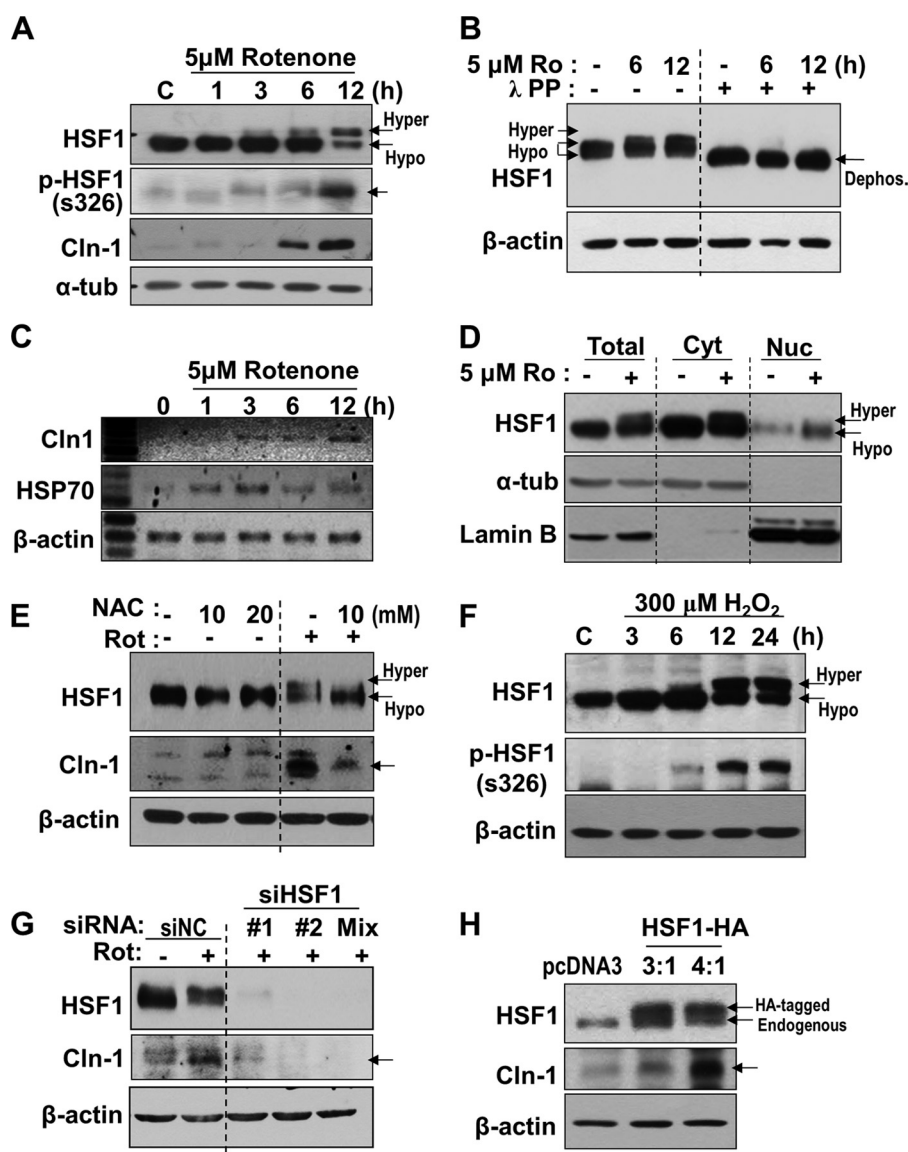


**FIGURE 4. Complex I inhibition induces Cln-1 expression by ROS-mediated HSF1 activation.** A–C, the Ch-L clone was treated with 5  $\mu$ M rotenone (Ro) for the indicated time periods. A, Western blot analysis. C, control;  $\alpha$ -tub,  $\alpha$ -tubulin. B, cell lysates were incubated with  $\lambda$  phosphatase for 2 h and subjected to Western blot analysis. Dephos, dephosphorylation. C, RT-PCR for mRNA levels. D, after the Ch-L clone was treated with 5  $\mu$ M rotenone for 12 h, nuclear (Nuc) and cytoplasmic (Cyt) fractions were isolated as described under “Experimental Procedures.” E, the Ch-L clone was exposed to 5  $\mu$ M rotenone for 12 h with or without pretreatment of NAC for 6 h and subjected to Western blot analysis. F, the Ch-L clone was exposed to 300  $\mu$ M H<sub>2</sub>O<sub>2</sub> for the indicated time periods and subjected to Western blot analysis. G, the Ch-L clone was transfected with siRNAs for HSF1 and then exposed to 5  $\mu$ M rotenone for 12 h. Cell lysates were subjected to Western blot analysis. H, the Ch-L clone was transfected with pcDNA-HSF1-HA for 2 days. Cell lysates were subjected to Western blot analysis.

HSF1 phosphorylation (activation) is involved in certain hepatoma cell invasiveness via Cln-1 expression.

## Discussion

Mitochondrial respiratory defects that are accompanied by mitochondrial gene mutations are common in most cancers (35, 36). Therefore, they are considered a metabolic hallmark of cancer. Although the contribution of mitochondrial defects to cancer development, such as tumor angiogenesis, metastasis, and chemoresistance, has often been reported (6, 10, 11, 37–39), it is unclear how mitochondrial impairment regulates tumor progression. One plausible explanation is that an altered mitochondrial metabolism communicates with the nucleus through “mitochondrial retrograde signaling.” The retrograde

signaling begins with the release of second messengers, ROS and Ca<sup>2+</sup>, from defective mitochondria (40). These messengers then activate several cytosolic signaling transducers through redox modification or posttranslational modification. In turn, certain transcription factors or cofactors are activated and/or trans-localize into the nucleus, switching on gene transcriptions *de novo* (40, 41). Therefore, the key molecular link between mitochondrial defects and tumor progression is the activation of certain transcription factors.

Several key transcription factors, including CREB and PGC-1, have been identified to regulate mitochondrial defect-responsive transcriptional reprogramming (40). In this study, we demonstrated that HSF1 is another mitochondrial retrograde-responsive transcription factor regulated by mitochon-



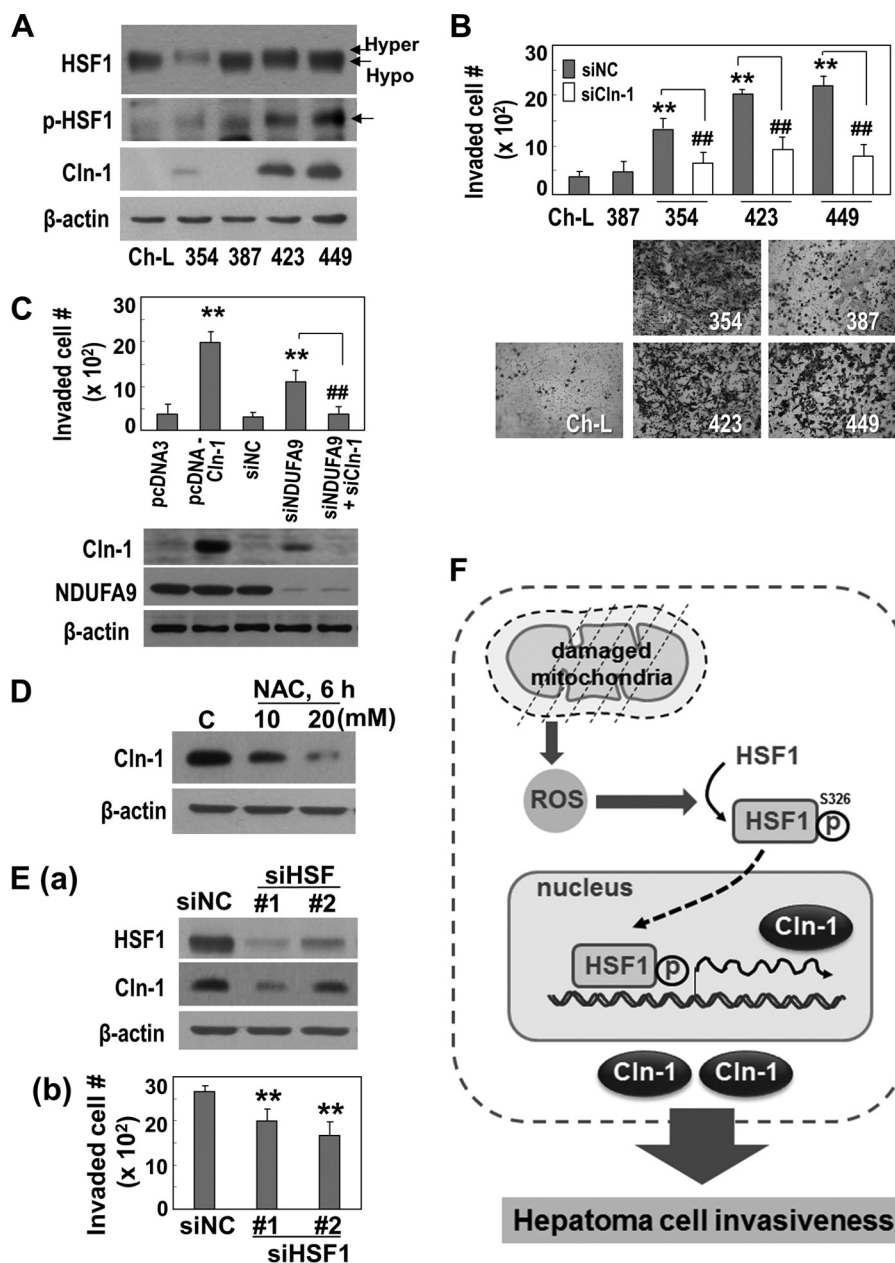


**FIGURE 6. HSF1 regulates hepatoma cell invasion activity through Cln1 expression.** *A*, Western blot analysis. *B*, SNU354, SNU423, and SNU449 cells were transfected with siRNA for Cln-1 for 2 days and subjected to a cell invasion assay. Representative images of invaded cells are shown in the *bottom panel*. *C*, the Ch-L clone was transfected with pcDNA-Cln-1, siNDUFA9, and/or siCln-1 for 2 days and then subjected to cell invasion activity (*top panel*) and Western blot analysis (*bottom panel*). *D*, SNU449 cells were treated with NAC for 6 h and subjected to Western blot analysis. *C*, control. *E*, SNU449 cells were transfected with siRNAs for HSF1 for 2 days and then subjected to Western blot analysis (*a*) and cell invasion activity (*b*). \* and #,  $p < 0.05$ ; \*\* and ##,  $p < 0.01$  versus control by Student's *t* test. *F*, schematic of the involvement of mitochondrial defect-induced HSF1 activation in Cln-1-mediated hepatoma cell invasiveness.

explanations for this unexpected finding are that the HSF1 trimer may bind three dispersed HSE sequences that are placed closely by the looping DNA strand or that binding of hyperphosphorylated HSF1 to a single HSE may activate the Cln-1 promoter with the help of other factors activated by mitochondrial defect-mediated retrograde signaling. In this way, HSF1 may regulate the transcription of various target genes, such as Cln-1, in addition to HSPs. However, if any inhibitory factors exist in some cellular context, then HSF1 activity on Cln-1 promoter may be invalid, as in the case of SNU423. These results contribute to a better understanding of the novel regulatory mechanism of HSF1.

Major targets of HSF1 are known to be HSPs, which restore the structures of proteins distorted by proteotoxic stress. Therefore, induction of HSPs by HSF1 under mitochondrial oxidative stress must be required to maintain essential cellular functions for tumor progression. However, it is still questionable why HSF1 activates Cln-1 transcription. Although recent studies support the involvement of Cln-1 in tumor metastasis, the detailed molecular mechanisms of how Cln-1 regulates tumor activities remain unclear. In general, tight junctions regulate the passage of ions and molecules through the paracellular pathway in epithelial and endothelial cells. However, Cln-1 also has unexpected roles in tumor cells. It recruits and promotes

## Mitochondrially Mediated HSF1 Activation Induces Cln-1

the activation of matrix metalloproteinase 2 and makes tumor cells aggressive (25). Interestingly, Cln-1 alone is sufficient to exert a tight junction-mediated gate function in metastatic tumor cells even in the absence of other tight junction-associated proteins (50). These findings suggest that Cln-1 may be required to overcome the cellular stress triggered by mitochondrial defects by exporting excess ions or stressors out of the cell. Our results from this study demonstrate that Cln-1 is up-regulated in response to mitochondrial ROS in the early stage of HCC invasiveness via HSF1 activation. The detailed molecular mechanisms of how Cln-1 controls HCC invasion activity remain to be elucidated.

**Author Contributions**—J. H. L., Y. K. L., and J. J. L. performed and analyzed most experiments, with assistance from H. O. B. for a few experiments. I. P. and G. H. K. performed a few experiments added to the revised version. W. G. X. and H. J. W. provided human hepatoma tissues and analyzed the results shown in Fig. 1, D and E. G. Y. designed and coordinated the study and wrote the paper.

### References

- Brandon, M., Baldi, P., and Wallace, D. C. (2006) Mitochondrial mutations in cancer. *Oncogene* **25**, 4647–4662
- Warburg, O. (1956) On the origin of cancer cells. *Science* **123**, 309–314
- Gatenby, R. A., and Gillies, R. J. (2004) Why do cancers have high aerobic glycolysis? *Nat. Rev. Cancer* **4**, 891–899
- Chatterjee, A., Mambo, E., and Sidransky, D. (2006) Mitochondrial DNA mutations in human cancer. *Oncogene* **25**, 4663–4674
- Nishikawa, M., Nishiguchi, S., Shiomi, S., Tamori, A., Koh, N., Takeda, T., Kubo, S., Hirohashi, K., Kinoshita, H., Sato, E., and Inoue, M. (2001) Somatic mutation of mitochondrial DNA in cancerous and noncancerous liver tissue in individuals with hepatocellular carcinoma. *Cancer Res.* **61**, 1843–1845
- Petros, J. A., Baumann, A. K., Ruiz-Pesini, E., Amin, M. B., Sun, C. Q., Hall, J., Lim, S., Issa, M. M., Flanders, W. D., Hosseini, S. H., Marshall, F. F., and Wallace, D. C. (2005) mtDNA mutations increase tumorigenicity in prostate cancer. *Proc. Natl. Acad. Sci. U.S.A.* **102**, 719–724
- Sotgia, F., Whitaker-Menezes, D., Martinez-Outschoorn, U. E., Salem, A. F., Tsigos, A., Lamb, R., Sneddon, S., Hulit, J., Howell, A., and Lisanti, M. P. (2012) Mitochondria “fuel” breast cancer metabolism: fifteen markers of mitochondrial biogenesis label epithelial cancer cells, but are excluded from adjacent stromal cells. *Cell Cycle* **11**, 4390–4401
- Dang, C. V., Kim, J. W., Gao, P., and Yuste, J. (2008) The interplay between MYC and HIF in cancer. *Nat. Rev. Cancer* **8**, 51–56
- Kim, J. H., Kim, H. Y., Lee, Y. K., Yoon, Y. S., Xu, W. G., Yoon, J. K., Choi, S. E., Ko, Y. G., Kim, M. J., Lee, S. J., Wang, H. J., and Yoon, G. (2011) Involvement of mitophagy in oncogenic K-Ras-induced transformation: overcoming a cellular energy deficit from glucose deficiency. *Autophagy* **7**, 1187–1198
- He, X., Zhou, A., Lu, H., Chen, Y., Huang, G., Yue, X., Zhao, P., and Wu, Y. (2013) Suppression of mitochondrial complex I influences cell metastatic properties. *PLoS ONE* **8**, e61677
- Ma, J., Zhang, Q., Chen, S., Fang, B., Yang, Q., Chen, C., Miele, L., Sarkar, F. H., Xia, J., and Wang, Z. (2013) Mitochondrial dysfunction promotes breast cancer cell migration and invasion through HIF1 $\alpha$  accumulation via increased production of reactive oxygen species. *PLoS ONE* **8**, e69485
- Guaragnella, N., Giannattasio, S., and Moro, L. (2014) Mitochondrial dysfunction in cancer chemoresistance. *Biochem. Pharmacol.* **92**, 62–72
- Weinberg, F., Hamanaka, R., Wheaton, W. W., Weinberg, S., Joseph, J., Lopez, M., Kalyanaram, B., Mutlu, G. M., Budinger, G. R., and Chandel, N. S. (2010) Mitochondrial metabolism and ROS generation are essential for Kras-mediated tumorigenicity. *Proc. Natl. Acad. Sci. U.S.A.* **107**, 8788–8793
- Lei, Y., Huang, K., Gao, C., Lau, Q. C., Pan, H., Xie, K., Li, J., Liu, R., Zhang, T., Xie, N., Nai, H. S., Wu, H., Dong, Q., Zhao, X., Nice, E. C., Huang, C., and Wei, Y. (2011) Proteomics identification of ITGB3 as a key regulator in reactive oxygen species-induced migration and invasion of colorectal cancer cells. *Mol. Cell. Proteomics* **10**, M110.005397
- Gorrini, C., Harris, I. S., and Mak, T. W. (2013) Modulation of oxidative stress as an anticancer strategy. *Nat. Rev. Drug Discov.* **12**, 931–947
- Hengstler, J. G., and Bolt, H. M. (2008) Oxidative stress: from modification of cell-cycle related events, secondary messenger function, dysregulation of small GTPases, protein kinases and phosphatases to redox-sensitive cancer models. *Arch. Toxicol.* **82**, 271–272
- Moreno-Sánchez, R., Rodríguez-Enríquez, S., Marín-Hernández, A., and Saavedra, E. (2007) Energy metabolism in tumor cells. *FEBS J.* **274**, 1393–1418
- Pelicano, H., Martin, D. S., Xu, R. H., and Huang, P. (2006) Glycolysis inhibition for anticancer treatment. *Oncogene* **25**, 4633–4646
- Sabharwal, S. S., and Schumacker, P. T. (2014) Mitochondrial ROS in cancer: initiators, amplifiers or an Achilles’ heel? *Nat. Rev. Cancer* **14**, 709–721
- Hung, W. Y., Wu, C. W., Yin, P. H., Chang, C. J., Li, A. F., Chi, C. W., Wei, Y. H., and Lee, H. C. (2010) Somatic mutations in mitochondrial genome and their potential roles in the progression of human gastric cancer. *Biochim. Biophys. Acta* **1800**, 264–270
- Michl, P., Barth, C., Buchholz, M., Lerch, M. M., Rolke, M., Holzmann, K. H., Menke, A., Fensterer, H., Giehl, K., Löhr, M., Leder, G., Iwamura, T., Adler, G., and Gress, T. M. (2003) Claudin-4 expression decreases invasiveness and metastatic potential of pancreatic cancer. *Cancer Res.* **63**, 6265–6271
- Rangel, L. B., Agarwal, R., D’Souza, T., Pizer, E. S., Ald, P. L., Lancaster, W. D., Gregoire, L., Schwartz, D. R., Cho, K. R., and Morin, P. J. (2003) Tight junction proteins claudin-3 and claudin-4 are frequently overexpressed in ovarian cancer but not in ovarian cystadenomas. *Clin. Cancer Res.* **9**, 2567–2575
- Yoon, C. H., Kim, M. J., Park, M. J., Park, I. C., Hwang, S. G., An, S., Choi, Y. H., Yoon, G., and Lee, S. J. (2010) Claudin-1 acts through c-Abl-protein kinase C $\delta$  (PKC $\delta$ ) signaling and has a causal role in the acquisition of invasive capacity in human liver cells. *J. Biol. Chem.* **285**, 226–233
- Miyamori, H., Takino, T., Kobayashi, Y., Tokai, H., Itoh, Y., Seiki, M., and Sato, H. (2001) Claudin promotes activation of pro-matrix metalloproteinase-2 mediated by membrane-type matrix metalloproteinases. *J. Biol. Chem.* **276**, 28204–28211
- Oku, N., Sasabe, E., Ueta, E., Yamamoto, T., and Osaki, T. (2006) Tight junction protein claudin-1 enhances the invasive activity of oral squamous cell carcinoma cells by promoting cleavage of laminin-5  $\gamma$ 2 chain via matrix metalloproteinase (MMP)-2 and membrane-type MMP-1. *Cancer Res.* **66**, 5251–5257
- Kim, J. H., Kim, E. L., Lee, Y. K., Park, C. B., Kim, B. W., Wang, H. J., Yoon, C. H., Lee, S. J., and Yoon, G. (2011) Decreased lactate dehydrogenase B expression enhances claudin 1-mediated hepatoma cell invasiveness via mitochondrial defects. *Exp. Cell Res.* **317**, 1108–1118
- Yu, J. S., and Kim, A. K. (2011) Wogonin induces apoptosis by activation of ERK and p38 MAPKs signaling pathways and generation of reactive oxygen species in human breast cancer cells. *Mol. Cells* **31**, 327–335
- Byun, H. O., Jung, H. J., Seo, Y. H., Lee, Y. K., Hwang, S. C., Hwang, E. S., and Yoon, G. (2012) GSK3 inactivation is involved in mitochondrial complex IV defect in transforming growth factor (TGF)  $\beta$ 1-induced senescence. *Exp. Cell Res.* **318**, 1808–1819
- Seo, Y. H., Jung, H. J., Shin, H. T., Kim, Y. M., Yim, H., Chung, H. Y., Lim, I. K., and Yoon, G. (2008) Enhanced glycogenesis is involved in cellular senescence via GSK3/GS modulation. *Aging Cell* **7**, 894–907
- Lee, Y. K., Yoon, H. G., Wang, H. J., and Yoon, G. (2013) Decreased mitochondrial OGG1 expression is linked to mitochondrial defects and delayed hepatoma cell growth. *Mol. Cell* **35**, 489–497
- Lee, H. W., Heo, C. H., Sen, D., Byun, H. O., Kwak, I. H., Yoon, G., and Kim, H. M. (2014) Ratiometric two-photon fluorescent probe for quantitative detection of  $\beta$ -galactosidase activity in senescent cells. *Anal. Chem.* **86**, 10001–10005
- Wang, K., Fang, H., Xiao, D., Zhu, X., He, M., Pan, X., Shi, J., Zhang, H., Jia, X., Du, Y., and Zhang, J. (2009) Converting redox signaling to apoptotic

- activities by stress-responsive regulators HSF1 and NRF2 in fenretinide treated cancer cells. *PLoS ONE* **4**, e7538
33. Xia, W., and Voellmy, R. (1997) Hyperphosphorylation of heat shock transcription factor 1 is correlated with transcriptional competence and slow dissociation of active factor trimers. *J. Biol. Chem.* **272**, 4094–4102
  34. Guettouche, T., Boellmann, F., Lane, W. S., and Voellmy, R. (2005) Analysis of phosphorylation of human heat shock factor 1 in cells experiencing a stress. *BMC Biochem.* **6**, 4
  35. Modica-Napolitano, J. S., and Singh, K. K. (2004) Mitochondrial dysfunction in cancer. *Mitochondrion* **4**, 755–762
  36. Singh, A. K., Pandey, P., Tewari, M., Pandey, H. P., and Shukla, H. S. (2014) Human mitochondrial genome flaws and risk of cancer. *Mitochondrial DNA* **25**, 329–334
  37. Hung, W. Y., Huang, K. H., Wu, C. W., Chi, C. W., Kao, H. L., Li, A. F., Yin, P. H., and Lee, H. C. (2012) Mitochondrial dysfunction promotes cell migration via reactive oxygen species-enhanced  $\beta$ 5-integrin expression in human gastric cancer SC-M1 cells. *Biochim. Biophys. Acta* **1820**, 1102–1110
  38. Chang, C. J., Yin, P. H., Yang, D. M., Wang, C. H., Hung, W. Y., Chi, C. W., Wei, Y. H., and Lee, H. C. (2009) Mitochondrial dysfunction-induced amphiregulin upregulation mediates chemo-resistance and cell migration in HepG2 cells. *Cell. Mol. Life Sci.* **66**, 1755–1765
  39. Shidara, Y., Yamagata, K., Kanamori, T., Nakano, K., Kwong, J. Q., Manfredi, G., Oda, H., and Ohta, S. (2005) Positive contribution of pathogenic mutations in the mitochondrial genome to the promotion of cancer by prevention from apoptosis. *Cancer Res.* **65**, 1655–1663
  40. Finley, L. W., and Haigis, M. C. (2009) The coordination of nuclear and mitochondrial communication during aging and calorie restriction. *Ageing Res. Rev.* **8**, 173–188
  41. Wallace, D. C. (2005) A mitochondrial paradigm of metabolic and degenerative diseases, aging, and cancer: a dawn for evolutionary medicine. *Annu. Rev. Genet.* **39**, 359–407
  42. Santagata, S., Hu, R., Lin, N. U., Mendillo, M. L., Collins, L. C., Hankinson, S. E., Schnitt, S. J., Whitesell, L., Tamimi, R. M., Lindquist, S., and Ince, T. A. (2011) High levels of nuclear heat-shock factor 1 (HSF1) are associated with poor prognosis in breast cancer. *Proc. Natl. Acad. Sci. U.S.A.* **108**, 18378–18383
  43. Shamovsky, I., and Nudler, E. (2008) New insights into the mechanism of heat shock response activation. *Cell. Mol. Life Sci.* **65**, 855–861
  44. Ciocca, D. R., Arrigo, A. P., and Calderwood, S. K. (2013) Heat shock proteins and heat shock factor 1 in carcinogenesis and tumor development: an update. *Arch. Toxicol.* **87**, 19–48
  45. Mendillo, M. L., Santagata, S., Koeva, M., Bell, G. W., Hu, R., Tamimi, R. M., Fraenkel, E., Ince, T. A., Whitesell, L., and Lindquist, S. (2012) HSF1 drives a transcriptional program distinct from heat shock to support highly malignant human cancers. *Cell* **150**, 549–562
  46. Fang, F., Chang, R., and Yang, L. (2012) Heat shock factor 1 promotes invasion and metastasis of hepatocellular carcinoma *in vitro* and *in vivo*. *Cancer* **118**, 1782–1794
  47. Jacquier-Sarlin, M. R., and Polla, B. S. (1996) Dual regulation of heat-shock transcription factor (HSF) activation and DNA-binding activity by H<sub>2</sub>O<sub>2</sub>: role of thioredoxin. *Biochem. J.* **318**, 187–193
  48. Yan, L. J., Christians, E. S., Liu, L., Xiao, X., Sohal, R. S., and Benjamin, I. J. (2002) Mouse heat shock transcription factor 1 deficiency alters cardiac redox homeostasis and increases mitochondrial oxidative damage. *EMBO J.* **21**, 5164–5172
  49. Guertin, M. J., Petesch, S. J., Zobeck, K. L., Min, I. M., and Lis, J. T. (2010) *Drosophila* heat shock system as a general model to investigate transcriptional regulation. *Cold Spring Harb. Symp. Quant. Biol.* **75**, 1–9
  50. Hoevel, T., Macek, R., Mundigl, O., Swisshelm, K., and Kubbies, M. (2002) Expression and targeting of the tight junction protein CLDN1 in CLDN1-negative human breast tumor cells. *J. Cell. Physiol.* **191**, 60–68